https://doi.org/10.5194/tc-2021-169
Preprint. Discussion started: 12 July 2021

The Cryosphere Discussions
Open Access
EGU

The potential of InSAR for assessing meltwater lake dynamics on Antarctic ice shelves

Weiran Li [1], Stef Lhermitte [1], and Paco López-Dekker [1]

[1]Department of Geoscience and Remote Sensing, Delft University of Technology, Delft, The Netherlands

Correspondence: Weiran Li (w.li-7@tudelft.nl)

Abstract. Surface meltwater drains on several Antarctic ice shelves, resulting in surface and sub-surface lakes that are potentially critical for the ice shelf collapse. Yet, our understanding and assessment of the drainage or refreezing of these lakes is limited, mainly due to lack of field observations and to the limitations of optical satellite imagery. Therefore, this paper explores the potential of backscatter intensity and of interferometric coherence and phase from C-band synthetic aperture radar (SAR) imagery as an alternative to assess the dynamics of meltwater lakes. In two case studies over Amery and Roi Baudouin ice shelves, we analyse i) the spatial and ii) the temporal variations of SAR backscatter intensity with iii) coherence and iv) interferogram phase (InSAR) patterns detected by Sentinel-1 data over multiple meltwater lakes. Throughout the year the lakes are observed in completely frozen state, in partially frozen state with a floating ice lid, and as open water lakes. The analysis reveals that the meltwater lake delineation is challenging during the melting period when the contrast between melting snow and lakes is confounded. On the other hand, it shows that the lake dynamics can be effectively captured during the refreezing process and the winter season by combining backscatter and InSAR information. In particular, the InSAR coherence and interferogram phase information are deemed essential throughout this whole period to distinguish between refrozen ice and subsurface meltwater. Additionally, the results provide significant evidence on the potential of the interferogram fringe patterns to detect and characterise instant events, such as lake drainage events over ice shelves. The potential of this technique to monitor these meltwater change events is however strongly determined by the satellite revisit interval and potential changes in scattering properties due to snowfall or melt events.

1 Introduction

Over the past decades, widespread surface meltwater has been spotted over multiple ice shelves in Antarctica (Kingslake et al., 2017) with potential far-reaching implications for hydrofracturing and ice-shelf collapse (Bell et al., 2018). Since meltwater lakes and ponds increase the gravitational load, depressing the ice shelf surface and inducing an uplift in the surrounding, the stress in the uplifting area can lead to fracture. On the contrary, a draining meltwater pond leads to a hydrostatic rebound, which also results in fracture (Banwell et al., 2013). The repeating filling and drainage process increases the vulnerability of the ice shelf to hydrofracture. Therefore, assessing the filling, drainage or refreezing of these lakes on Antarctic ice shelves is key to understanding the response of Antarctica in a future climate.

https://doi.org/10.5194/tc-2021-169
Preprint. Discussion started: 12 July 2021

Satellite remote sensing has been the major tool to delineate supra-glacial lakes and assess surface meltwater dynamics, given the remote location, large extent, and harsh conditions that limit extensive field observations on Antarctica. Previous studies exploited various satellite remote sensing data sources, including optical and synthetic aperture radar (SAR) imagery. For example, Kingslake et al. (2017) provided an overview of the Antarctic-wide meltwater hydrological network by combining Landsat, WorldView and Aster satellite imagery in combination with aerial photography. A study from Lenaerts et al. (2016) detected meltwater features on the Roi Baudouin Ice Shelf (RBIS) using a combination of optical Landsat imagery and L-band radar imagery from the ALOS/PALSAR instrument, which is capable of mapping subsurface meltwater. Optical imagery (e.g. Landsat-8) and C-band SAR imagery (e.g. Sentinel-1 in HH and/or HV polarisation) are combined to detect subsurface meltwater in (Miles et al., 2017) and lake drainage in (Benedek and Willis, 2021) in Greenland and Antarctica (Dunmire et al., 2020), whereas Dirscherl et al. (2021) used deep learning techniques on Sentinel-1 HH backscatter intensities for automated supraglacial lake mapping across Antarctica.

Despite the potential of optical imagery and SAR data in detecting and monitoring surface meltwater, both methods have limitations over Antarctica. Polar nights and cloud cover limit data availability from visible-band and near-infrared imagery (Selmes et al., 2013; Williamson et al., 2017), which is not the case for Sentinel-1 SAR data. The cross-polarised backscatter intensity (HV or VH) provides on average a better contrast between water and ice than HH polarisation (Miles et al., 2017), but it is not always available over Antarctica. Interpreting radar imagery moreover may not be that straightforward as snow (Fahnestock et al., 1993) and meltwater features (Miles et al., 2017) in SAR images can result in ambiguous signals.

The ambiguity in meltwater lake features SAR imagery is the result of the combination of dielectric properties and geometry, which both determine the backscatter intensity and which can be related to multiple factors including wetness, roughness and snow grain size (Fahnestock et al., 1993). For example, both dry snow and bare ice typically show low backscatter intensities due to limited volume scattering and specular reflection over the blue ice area. A melting snow/firn surface or open lake, however, also results in low backscatter intensities due to the increased absorption due to change in dielectric constant (Ulaby et al., 1981; Nagler et al., 2016). Refrozen snow/firn with large snow grains, on the other hand, result in strong backscatter intensities due to the high volume scattering (Fahnestock et al., 1993), but can be easily confounded with rough surfaces or ice lids that also result in high backscatter intensities due to the roughness or the high dielectric contrast between the ice lid and water below (Hirose et al., 2008; Antonova et al., 2016). The meltwater features may moreover change over time resulting in variable backscatter intensity signatures. Complete refreezing of a lake, for example, may result in the disappearance of the high dielectric contrast between the ice lid and water below, resulting in a decrease in backscatter intensity (Hirose et al., 2008).

A potential solution to these limitations is interferometric processing of the synthetic aperture radar data (InSAR) which provides complementary information on the geometric and dielectric properties of the meltwater features. Repeat-pass InSAR method processes pairs of images of the same area separated by a certain time to derive coherence and interferometric phase information. The coherence can be considered as an indicator for changes in the relative position of the scatterers between the two acquisitions, whereas the interferometric phase measures their average range difference from the satellites. For high coherence areas, the phase can be related to a line-of-sight displacement without change in scattering properties, whereas for low coherence areas, the phase becomes scarcely informative (Hanssen, 2001). This combination of coherence and phase

https://doi.org/10.5194/tc-2021-169
Preprint. Discussion started: 12 July 2021

information from InSAR is expected to facilitate the continuous monitoring of meltwater dynamics. For example, in absence of changes in scattering due to changing snow/ice conditions or intense regional melts, the coherence of the InSAR images should be generally high. However, when lakes drain or refreeze, the scattering properties will change, reducing the coherence of the InSAR images. These changes in InSAR coherence have been proven useful in X-band for monitoring the refreeze of thermokarst lakes in the Arctic region (Antonova et al., 2016). So far, however, no analysis has been conducted for C-band time-series. Additionally, the interferometric phase might reveal information about the drainage and filling of lakes as these processes basically result in a vertical displacement of the surface (Banwell et al., 2013). However, the added value of InSAR for such applications has not been tested or quantified yet.

The objective of this paper is to assess the potential of C-band InSAR data to quantify the dynamic behaviour of meltwater filling, drainage and refreezing. For this purpose we use a combination of backscatter intensities and InSAR information from the Sentinel-1 mission to monitor the meltwater over two Antarctic ice shelves (i.e. Roi Baudouin Ice Shelf (RBIS) and Amery Ice Shelf (Amery)) as case studies where we have optical satellite data as additional reference data.

2 Data & Methods

2.1 Study areas

Two ice shelves in East Antarctica with well known meltwater dynamics (Kingslake et al., 2017) have been used as case studies for this study. The first case study is on the Roi Baudouin Ice Shelf (RBIS), where in situ research has been conducted and the exact locations of several lakes were mapped during a field campaign in Jan./Feb. 2016 (Lenaerts et al., 2016), which were revisited in Nov. 2017 when their lake collapse has been observed (Dunmire et al., 2020). In the RBIS case study, we used the supraglacial and englacial lakes mapped by Lenaerts et al. (2016) as delineated meltwater lake features and complemented that data set with manually delineated sample polygons of snow and ice surfaces based on Landsat imagery (Fig. 1).

For the second case study over Amery ice shelf, we used a similar approach based on sample lake, snow and ice sample regions. For Amery, however, a reference lake data set was not available. Therefore, lakes samples were mapped manually based on available Landsat-8 imagery in summer 2017-2018. The goal of this sampling was not to map all possible lakes, but to get a representative sample polygon for each snow/ice/lake class. Our lake class, however, overlaps with the lakes as mapped by Spergel et al. (2021).

2.2 Data

Two types of Level-1 Sentinel-1 Interferometric Wide (IW) products are used in this study: Single Look Complex (SLC) products, consisting of complex-valued data that preserve the phase information of the returned echoes, and Ground Range Detected (GRD) products, consisting of multi-looked backscatter intensity without phase information. For both products HH-polarisation was used as this is the only polarisation widely available over Antarctica. The GRD data were downloaded from the Google Earth Engine (GEE), whose processing includes thermal noise removal, radiometric calibration, and terrain correction.

https://doi.org/10.5194/tc-2021-169
Preprint. Discussion started: 12 July 2021

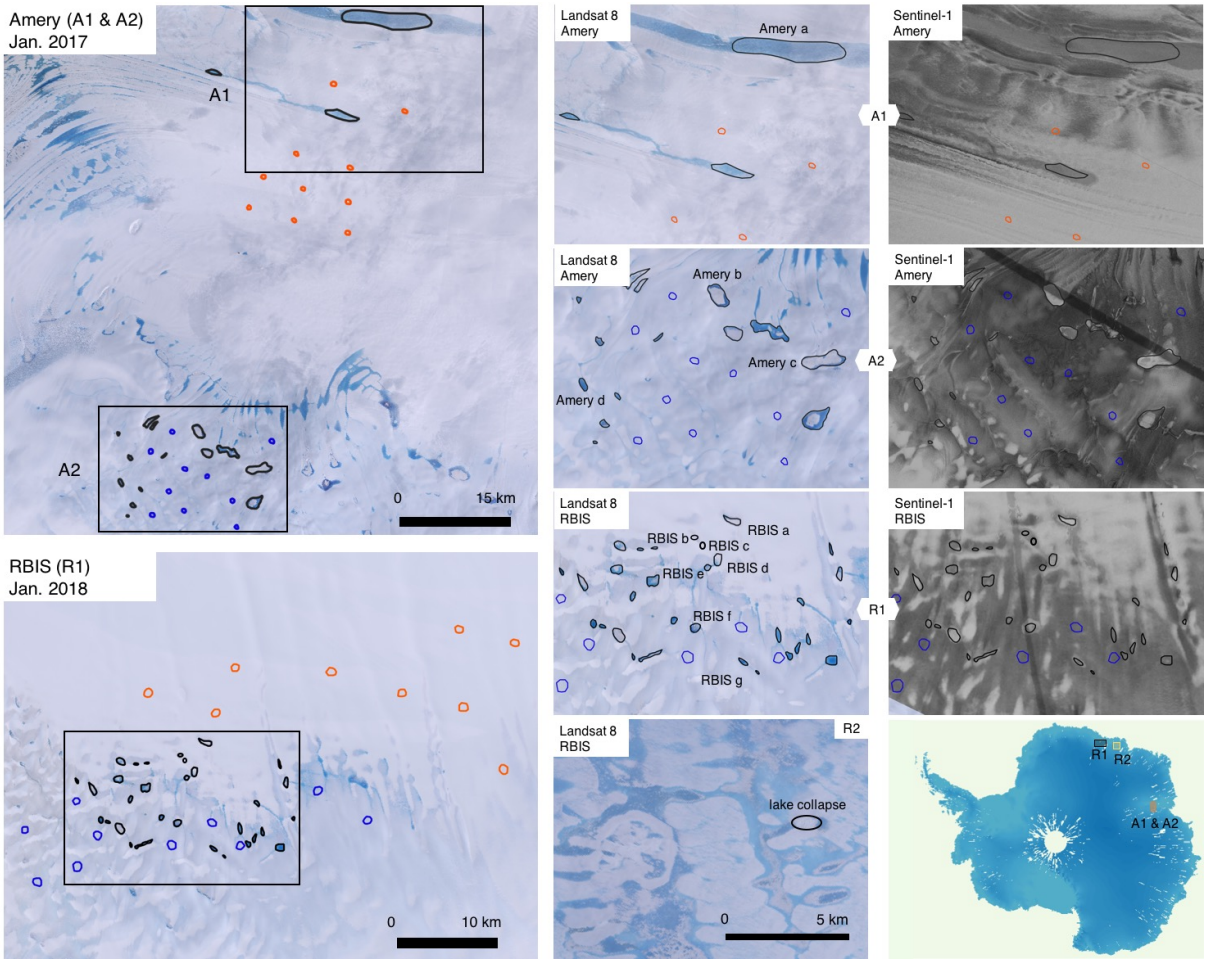

Figure 1. Outline of the Amery and RBIS study areas (referred to as A1, A2, R1, and R2). Close-ups of the investigated meltwater features are shown in both Landsat 8 images and Sentinel-1 backscatter intensities. In all panels the lakes used for the temporal backscatter and coherence analysis are delineated in black curves. The indices of the lakes correspond to the time series in Fig. 2. Snow (in orange) and ice (in blue) are also delineated as comparison for backscatter intensities and coherence. Panel R2 illustrates the lake feature selected for the interferogram analysis. The analysed locations are highlighted in the Antarctica map. The DEM used as the background is from the REMA project (Howat et al., 2019).

https://doi.org/10.5194/tc-2021-169
Preprint. Discussion started: 12 July 2021


The Cryosphere Discussions
Open Access
EGU

Table 1. List of the imagery used for the study. When the end date is not specified, the table entry refers to a single acquisition.

Ice shelf	Product	Track No.	Starting date	End date	Repeat cycle
RBIS	Sentinel-1 IW SLC	Ascending 59	2017/07/25	2018/04/15	12 days
RBIS	Sentinel-1 IW SLC	Descending 136	2017/12/04	2018/04/15	12 days
RBIS	Sentinel-1 IW GRD	Multiple	2016/06/01	2018/05/31	N/A
RBIS	Landsat 8	Path 157 Row 110	2017/09/26	-	N/A
RBIS	Landsat 8	Path 155 Row 110	2017/12/01	-	N/A
RBIS	Landsat 8	Path 153 Row 110	2017/12/19	-	N/A
RBIS	Landsat 8	Path 156 Row 110	2018/01/09	-	N/A
Amery	Sentinel-1 IW SLC	Descending 3	2017/01/04	2018/01/17	12 or 6 days
Amery	Sentinel-1 IW GRD	Multiple	2015/11/29	2018/05/31	N/A
Amery	Landsat 8	Path 127 Row 111	2017/01/27	-	N/A
Amery	Landsat 8	Path 126 Row 111	2017/10/03	-	N/A
Amery	Landsat 8	Path 127 Row 111	2018/01/14	-	N/A

The final backscatter product has a 20 m×20 m resolution. When normalised by the area of the resolution cell on the ground, the calibrated backscatter intensities are usually recalled as Normalized Radar Cross Sections (NRCS) and this is the term we will use for the remaining of the paper for backscatter intensity.

The Sentinel-1 SLC data were downloaded from the Copernicus Open Access Hub (Copernicus, 2017) and processed to derive phase information and NRCS. SLC processing and georeferencing were carried out using the Delft Object-oriented Radar Interferometric Software (DORIS) based on TanDEM-X digital elevation model (DEM) for RBIS (Lenaerts et al., 2016) and WGS84 geoid for Amery. The final SLC products have an azimuth resolution of 20 m and a ground range resolution of 5 m (Torres et al., 2012).

Additionally, Landsat 8 imagery was used as evaluation dataset to help interpreting the Sentinel-1 SAR data. For this purpose, available Landsat images were processed on the GEE. Detailed data type and acquisition dates are provided in Table 1.

2.3 Methods

To assess the potential of SAR backscatter intensities and InSAR coherence and phase for assessing meltwater lake dynamics we analyse the spatial and the temporal variations of Sentinel-1 backscatter intensity. Therefore, we compare the spatial and temporal characteristics of the identified lakes with their surroundings to assess how well they can be distinguished in different seasons. For this purpose the temporal variations in NRCS are first compared per lake, snow, ice class and for the individual lakes. Second, the spatio-temporal variation in NRCS is analysed along mono-dimensional transects across the largest lake dimension to assess the seasonal differences between the lakes and their surrounding areas. Subsequently, the NRCS changes are compared to changes in coherence and phase to assess the added value of combining NRCS, coherence and phase information to improve the understanding of the melt-refreeze process of lakes.

https://doi.org/10.5194/tc-2021-169
Preprint. Discussion started: 12 July 2021

110 # 3 Results

3.1 Backscatter intensity analysis

The NRCS time series of the lakes, snow and ice polygons show a strong seasonal variation, as the local snow/ice properties and the status of the lakes change over time (Fig. 2). The results on Amery ice shelf show that the NRCS decreases from snow (∼0 dB) to lakes (∼-5 dB) and ice (∼-10 dB) during fall, winter, spring, with the exception of the summer melt season (January
115 and February) when the NRCS of (wet) snow and lakes shows a strong drop in NRCS due to the change in dielectric constant as a result of melting. The individual highlighted lakes (Amery a, Amery b and Amery d) show sightly different temporal behaviour with drops in NRCS during the melt season, followed by NRCS increase after the melting season. For Amery a and Amery d this increase results in a temporary overshoot until reaching the winter NRCS level again.

The NRCS time series on RBIS show a similar pattern (i.e., $NRCS_{snow} > NRCS_{lake} > NRCS_{ice}$ between Feb. and Dec.)
120 except for Jan. 2018, where the $NRCS_{snow}$ drops below the $NRCS_{lake}$ and $NRCS_{ice}$. Some individual lakes also show a different behaviour than the mean lake time series. Lakes RBIS a, for example, which is located in a snow/firn area, shows a high backscatter between July and Dec. 2017 (similar to snow), but subsequently only recovers slowly, while the RBIS f and g show a temporal NRCS behaviour that more closely resembles the ice class. Both the Amery and RBIS time series show however that the discrimination of lakes based NRCS alone is not straightforward as the NRCS of the lakes often resembles
125 the NRCS of snow and ice.

A similar confusion between lakes and snow/ice samples is visible in the spatio-temporal analysis of the transects. Both the RBIS a and Amery d transect time series show again a significant inter-annual variation (Fig. 3). For RBIS a this starts with high NRCS values (similar to snow) with limited spatial variation in June - Nov. 2016, followed by a strong area wide decrease in NRCS during the melting season (Dec. 2016 - Feb. 2017). After this, a clear spatial pattern emerges with borders
130 of low NRCS and inner areas of high NRCS, followed again by a new area wide decrease in NRCS in the Dec. 2017 - Jan. 2018 melting season. This development is consistent with the description of ice lids in (Antonova et al., 2016) and the potential development of ice lids in winter on RBIS (Dunmire et al., 2020).

For Amery d, these spatio-temporal transect patterns of the lakes are less distinguishable from the ice area surroundings as the NRCS closely resembles the NRCS of the surrounding ice, except for Mar.-May 2018 when it shows a strong increase.

135 3.2 Coherence analysis

The coherence time series show a completely different behaviour than the NRCS time series (Fig. 2). On the Amery ice shelf, for example, snow, ice and lakes all have low or null coherence in summer, because of the altering scattering properties due to melt water content. For the ice and snow zones, the coherence rises abruptly when the surface refreezes in spring, while the coherence over the lakes rises only gradually until winter, when the lakes reach coherence values that are similar to snow and
140 ice. During winter, the coherence levels from snow, ice and lakes show a similar behaviour with large temporal variations when the coherence suddenly drops (i.e. fluctuating between 0.2 and 0.8 on 6 day time spans). These sudden drops are probably due

https://doi.org/10.5194/tc-2021-169
Preprint. Discussion started: 12 July 2021

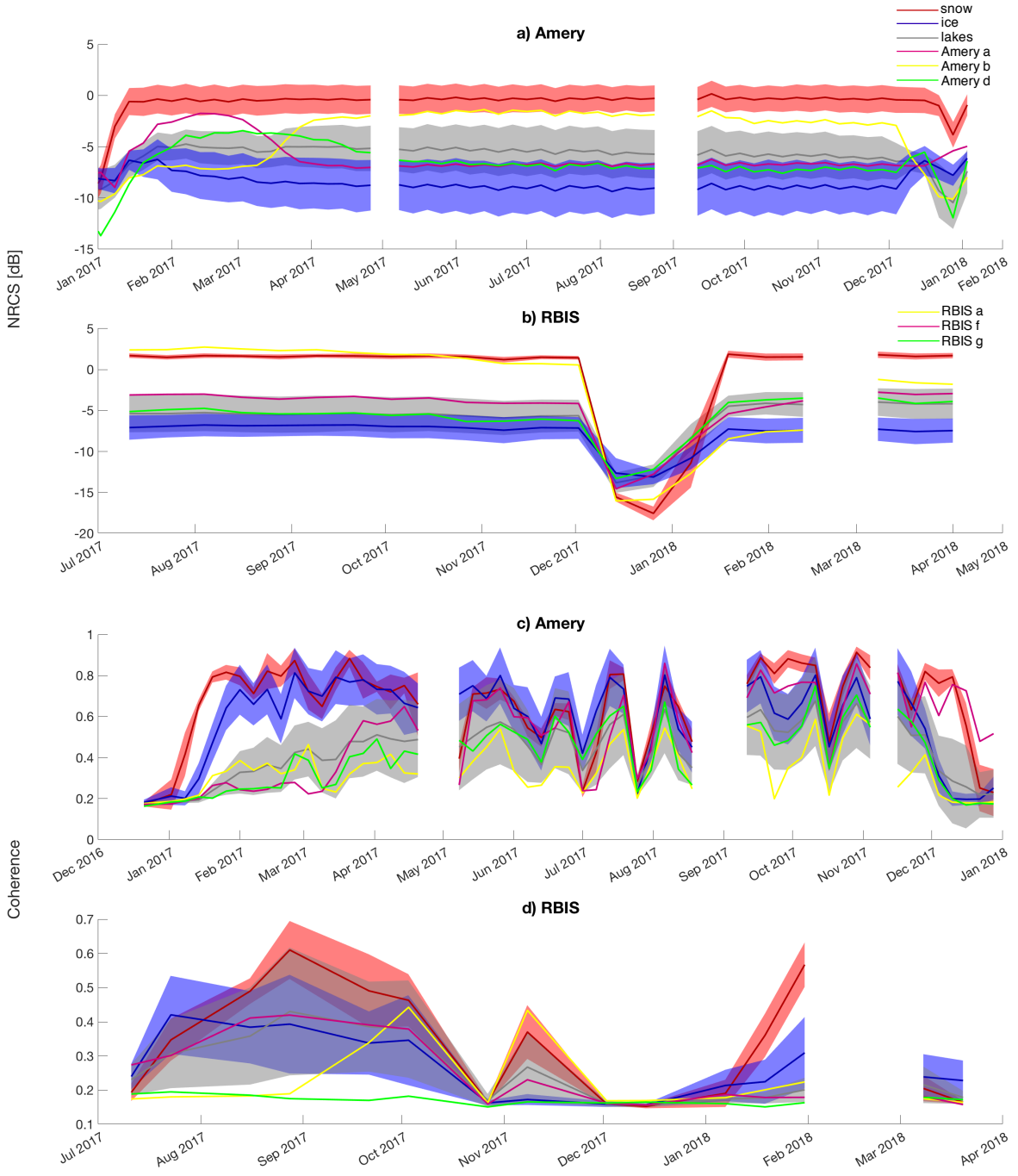

Figure 2. Time series of mean (solid line) and standard deviation (semi-tranparent area) of NRCS and coherence over selected polygons Amery and RBIS ice shelves in Fig. 1. Moments with lack of 6/12-day revisit frequency are masked, resulting in discontinuities.

https://doi.org/10.5194/tc-2021-169
Preprint. Discussion started: 12 July 2021

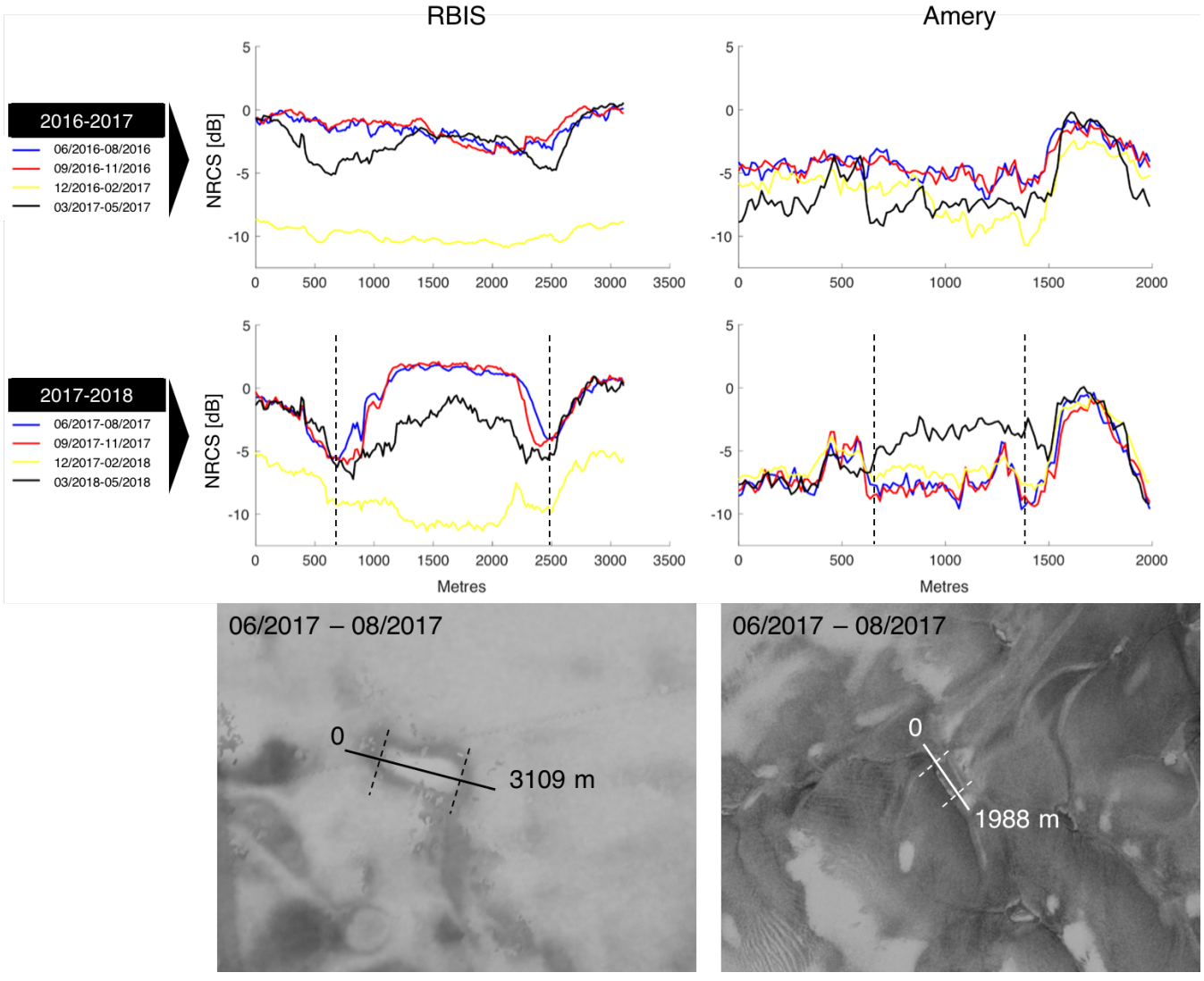

Figure 3. Spatial variation of Sentinel-1 NRCS for two different lakes: RBIS a (see Fig. 1) on the left and Amery d on the right. The upper and middle panels show the mean backscatter intensities over the lake transect for the June 2016 to May 2017 and for the June 2017 to May 2018 periods respectively. Each curve represents the average NRCS over a quarter year acquisitions. The transects as well as the 2D winter appearance of the feature surroundings are illustrated in the bottom panels.

https://doi.org/10.5194/tc-2021-169
Preprint. Discussion started: 12 July 2021

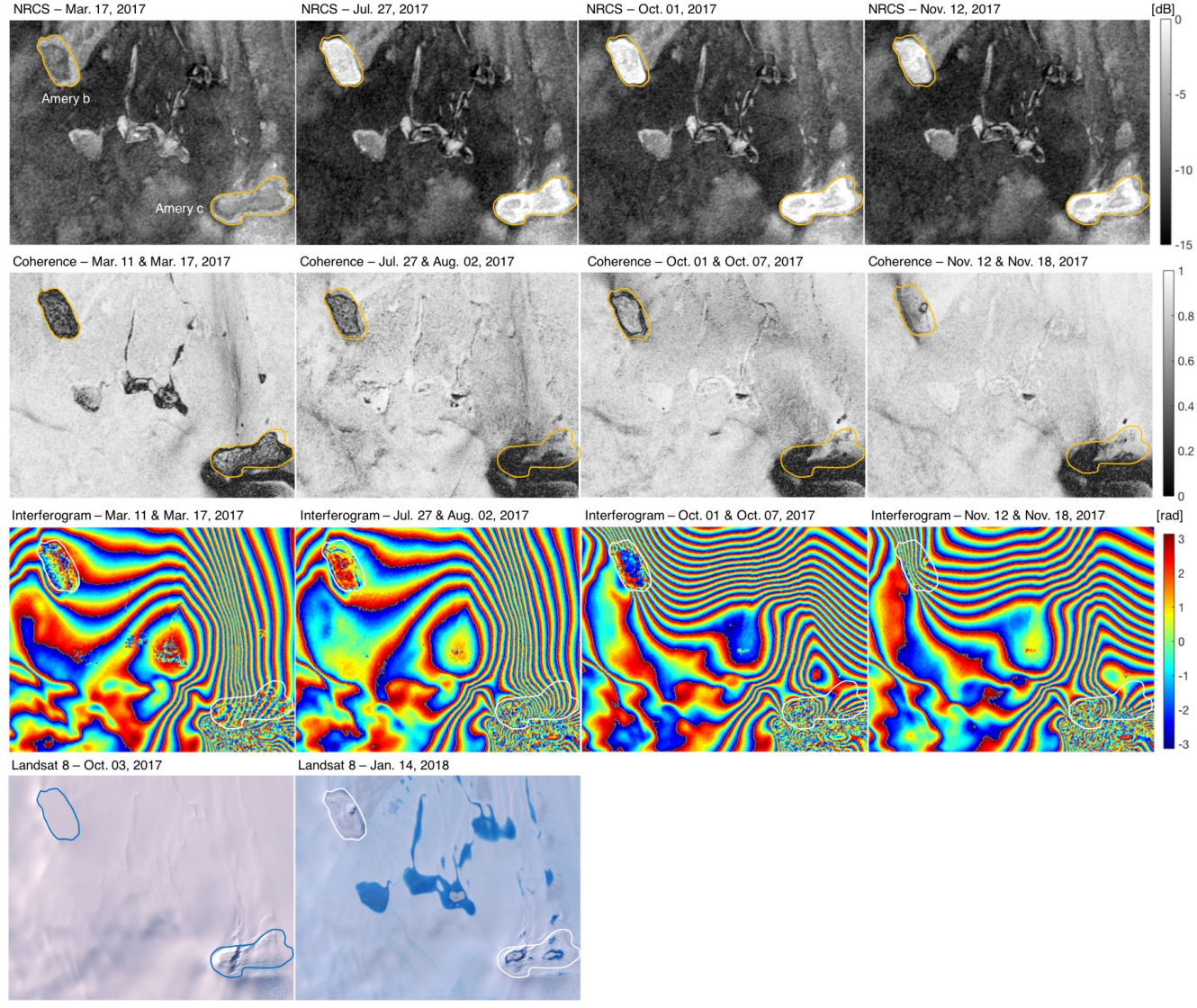

Figure 4. Synoptic outline for two lakes of interest on the Amery (referred to as Amery b and c). The NRCS, the coherence and the associated interferograms are shown for four representative dates throughout the year. The fringes in the background of the interferograms show the ice velocity and may indicate tidal movement. Two Landsat images are also shown to aid the visual interpretation of the radar features.

https://doi.org/10.5194/tc-2021-169
Preprint. Discussion started: 12 July 2021

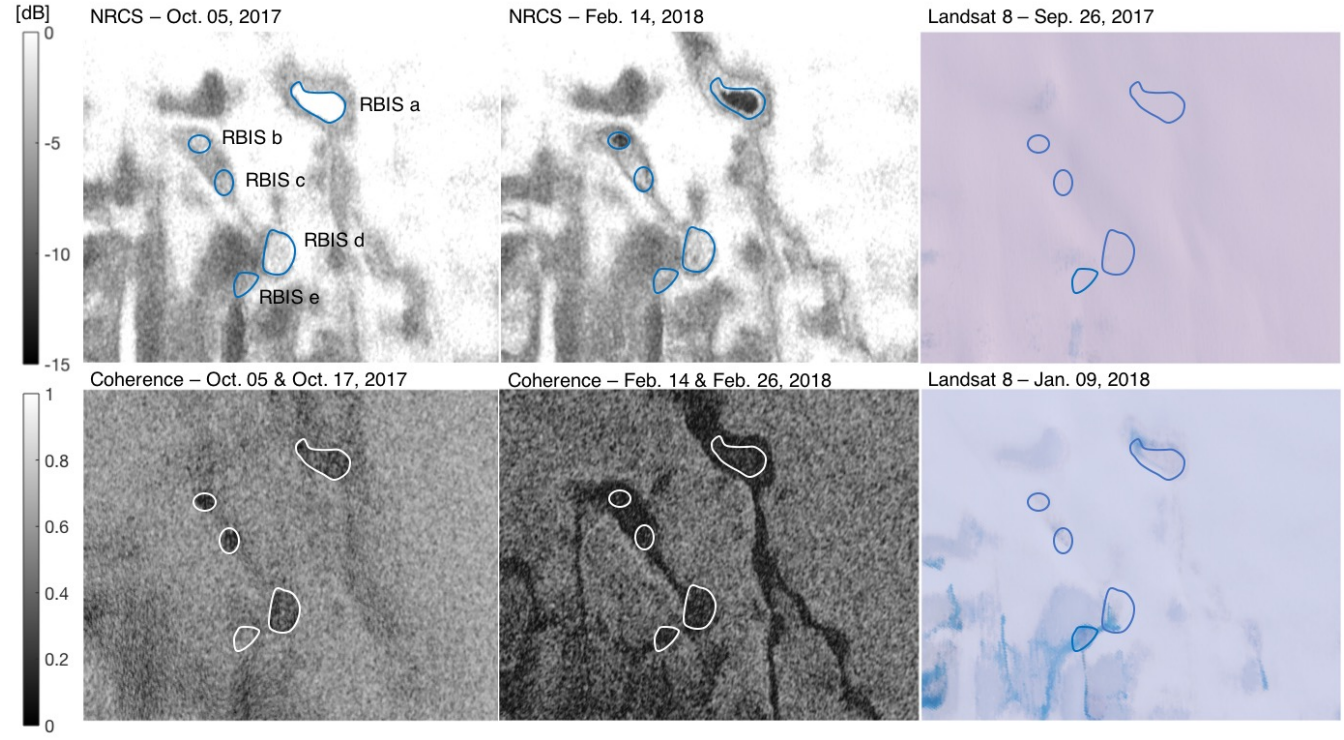

Figure 5. Coherence and NRCS in the RBIS region right before (left panels) and during (centre panels) the surface melt in the vicinity of RBIS a in the panels (c) of Fig. 1. These lakes are hereby referred to as RBIS a to e. Two cloud-free Landsat images close to the radar acquisitions are also reported in the right panels.

to weather-induced changes in scattering properties (e.g. after a snowfall event). These drops are however sparse as the 6-day revisit cycle allows to get good overall coherence.

On RBIS, on the other hand, the coherence is lower as the Sentinel-1 data are only available in a 12-day revisit cycle, which reduces the overall coherence and makes interpretation more complicated as more weather-induced changes in scattering properties could occur in a 12-day revisit. Despite the overall lower coherence, also on RBIS the coherence time series show a relatively stable period from August to October, with coherence values above 0.35. From Nov. 2016 to Jan. 2017, the coherence drops drastically, with an almost null coherence for all polygons. The coherence then increases again when the snow and ice surfaces refreeze in February. Overall, snow reaches the highest coherence (0.5-0.6), while the lakes show the lowest coherence. Lakes RBIS a and RBIS f however showed significant coherence values (0.4) during the winter season (only occasionally for RBIS a), while RBIS g presented null values throughout the whole year. This difference in behaviour could indicate differences in refreezing status.

To better understand the NRCS and coherence times series, some representative lake features in the Amery and RBIS zones are analysed in more detail in Fig. 4 and Fig. 5. The outlined lakes on Amery in Fig. 4 are characterised by dominant blue

https://doi.org/10.5194/tc-2021-169
Preprint. Discussion started: 12 July 2021

ice cover with low backscatter intensities, as conveyed by the dark background in the NRCS panels. The ice is intermittently covered by a shallow snow layer (e.g. Landsat image of Oct. 2017) which melts away in summer (e.g. Landsat image of Jan. 2018). This results in a stable ice surface with high coherence values. The lakes, on the other hand, show a more variable behaviour with lower coherence and strong changes in NRCS as a result of varying scattering properties. At the end of the summer (Mar. 2017), both lakes show a low NRCS whereas it becomes substantially brighter in the subsequent acquisitions from July to Nov. 2017. This corresponds to the observed NRCS increase Apr. 2017 for Amery b in Fig. 2. The NRCS and coherence signal is moreover not uniform across each lake with the appearance of polygonal features that show large differences between the centre of the lake (with higher NRCS and coherence) and a thin strip at the edges (with lower NRCS and coherence). This is consistent with earlier observations based on optical satellite imagery where the lakes show a circular appearance with a thick snow/ice lid in the center and ice/water at the edges (e.g., Fig. S1 in Dunmire et al., 2020). This pattern often changes over time as for example in the lake Amery c (Fig. 4), where the coherence increases for half of the lake and not for the other half, which could be an indicator of gradual non-spatially uniform refreezing or drainage. One example of such a drainage event could be seen in the small circular feature in the coherence of Amery b in Nov. 2017, which clearly corresponds to a collapsed circular feature in the Jan. 2018 Landsat imagery.

On RBIS the lakes are located in an area that contains both snow/firn regions region and blue ice. Since the Sentinel-1 SLC temporal coverage is lower than for Amery, SLC coverage only started in July 2017 (Fig. 5). The lake RBIS a shows a high NRCS in October and a low NRCS in February, which contrasts with the surroundings. The other lakes show a smaller contrast with their surroundings with intermediate NRCS values. The whole area frequently underwent coherence losses, especially in winter (Fig. 2d), possibly due to the 12-day revisit time. In Oct. 2017 and Feb. 2018, however, coherence is higher (>0.35). In both coherence image pairs, the meltwater features, with low or null coherence values, are sharply emerging from the background. In Feb. 2018, the coherence pairs moreover highlight a hydrological connection between the lakes, which is not straightforward to see in the NRCS or optical imagery. This highlights the increased potential for coherence over the backscatter intensity in delineating the lake network.

3.3 Interferogram analysis

The interferogram phases (Fig. 4) emphasise the differences in spatial cover and melting patterns between the two lakes on Amery ice shelf. The centre of Amery b shows fringes in all the acquisitions, even in March, despite the relatively low coherence. Between Mar. 2017 and Oct. 2017 the fringes are however disconnected from the fringes of the surroundings, whereas they connect seamlessly in November 2017. This pattern is consistent with lower coherence at the edges. Both the fringe discontinuity and coherence increase between Oct. and Nov. indicate the presence of meltwater until Oct. 2017, followed by a lake refreeze or drainage in Nov. The Landsat images show a smooth snow covered surface in Oct. 2017 and a rough doline-like surface in Jan. 2018. This supports the hypothesis that the lake drained and the surface collapsed and highlights the potential of coherence and interferogram analysis for analysing meltwater dynamics.

On the eastern part of RBIS, the interferogram shows a different potential for analysing meltwater dynamics (Fig. 6) as it shows a phase reversal (i.e. reversing the colour scheme in the interferogram panels) over the lake area in Dec. 2017 vs. a

https://doi.org/10.5194/tc-2021-169
Preprint. Discussion started: 12 July 2021

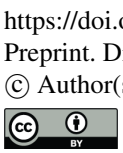

continuous phase in Apr. 2018. This phase reversal indicates that the lake has a displacement in the satellite line-of-sight which is opposite to the rest of the ice shelf. As the ice shelf background fringes correspond to the ice flow, in this case moving away from the satellite line-of-sight, the lake fringes indicate an uplift as a result of ice shelf rebounce after lake collapse. This would be consistent with rebound effects as described in Banwell et al. (2013). Indirect indicators of this lake collapse can also be observed in the Landsat 8 images before/after the collapse as the roughness of the surface strongly increased after collapse.

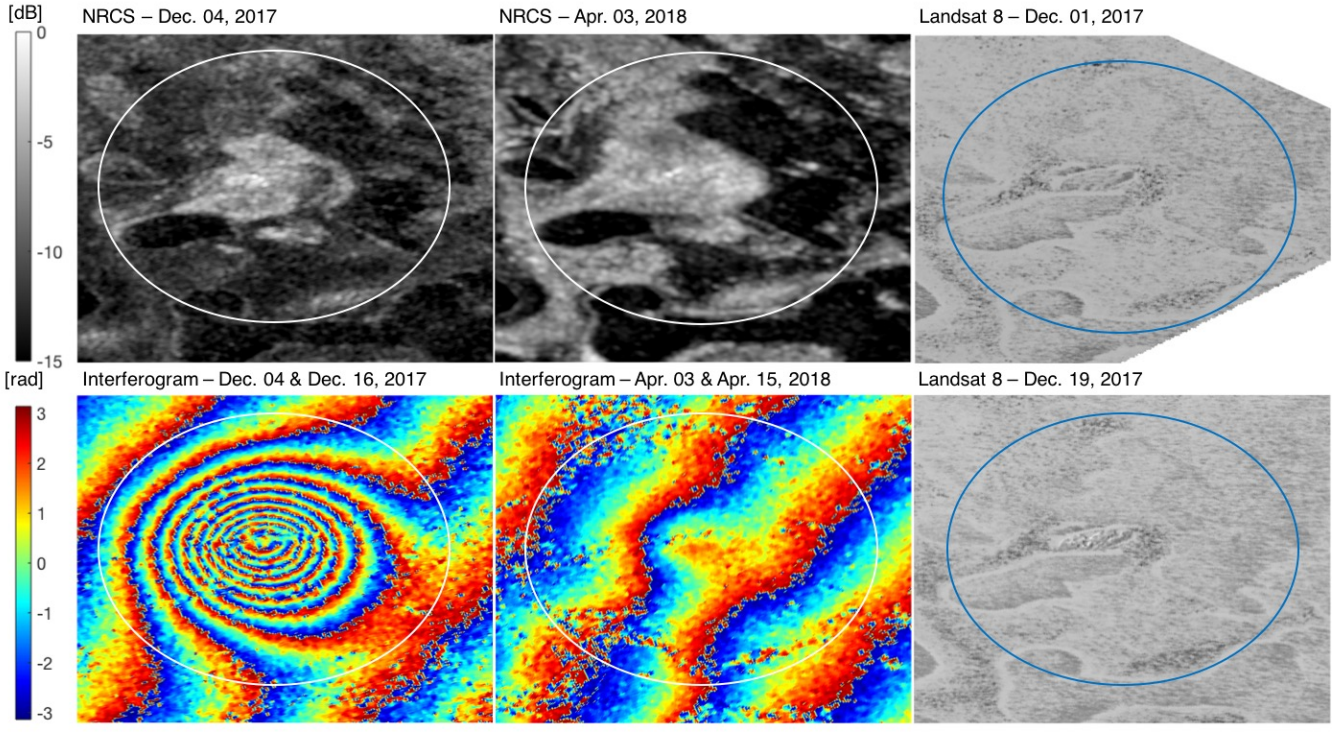

Figure 6. NRCS and interferogram phases for a lake feature in the east of the RBIS experiencing drainage in December 2017 (left panels) and ice-cover collapse in April 2018 (centre panels). Two Landsat 8 panchromatic images in correspondence of the two events are also shown (right panels).

Another potential of interferogram time series is the detection of lake refreezing as can be observed for the large lake feature in the middle of the Amery, labelled as Amery a in Fig. 1. Both Amery a and the surrounding ice shelf show an overall low NRCS and a complete incoherent interferogram on Jan. 4, 2017 (Fig. 7) as a result of surface melt. In subsequent weeks the NRCS and coherence of the snow surrounding area increase due to the refreezing as can be seen from the visible regular fringes. For the lake, however, this increase in coherence lags behind and only recovers slowly as more portions of the lake start to refreeze. During the refreezing, the fringes patterns over the lake gradually recover while the incoherent noise gradually diminishes. This pattern corresponds closely with the refreezing pattern identified by (Spergel et al., 2021) who also identified a gradual refreezing starting at the edges over 66 days based on transition from high-to-low backscatter intensity only. The

https://doi.org/10.5194/tc-2021-169
Preprint. Discussion started: 12 July 2021

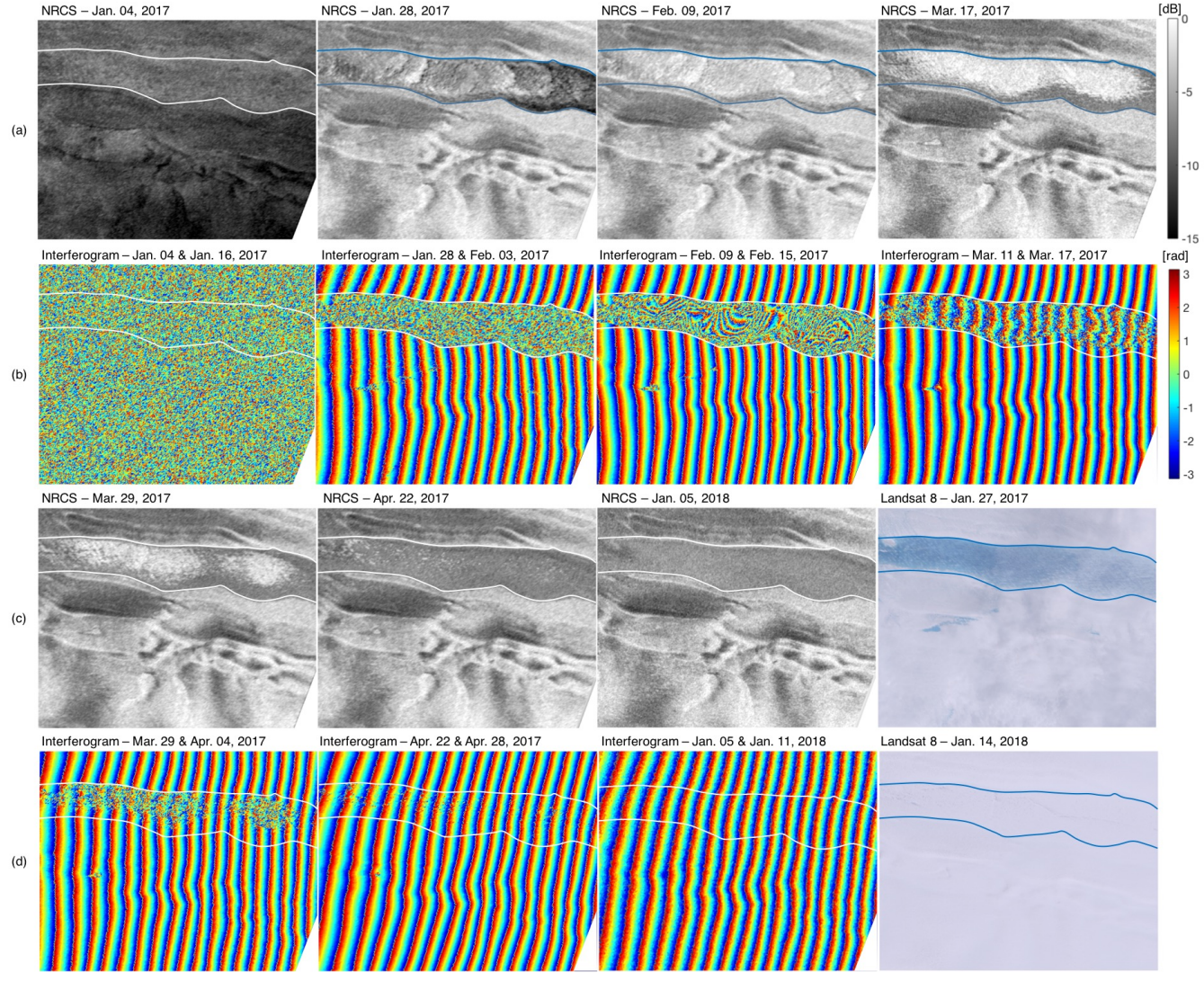

Figure 7. NRCS and interferogram phases for a large lake in the middle of the Amery region experiencing a refreezing process. The NRCS refers to the first image of the interferogram pairs. The interferograms clearly show that the lake refreezing occurs in the first half of 2017. The lake remains frozen throughout the remainder of 2017 and in 2018. The two Landsat 8 images in the lower right corner provide a visual evaluation.

https://doi.org/10.5194/tc-2021-169
Preprint. Discussion started: 12 July 2021

interferogram shows similar results here, but with the added value that the interpretation of high-low backscatter compared to the surroundings is less ambiguous.

4 Discussion

The different case studies provide an overview of the potential and shortcoming of backscatter intensity and coherence to assess meltwater lake dynamics. Low backscatter intensities can indicate blue ice areas or strong absorption due to meltwater, while high backscatter intensities indicate rough surfaces or strong volume scattering due to larger refrozen snow grains. The partly frozen lakes show moreover often a bright centre (high NRCS) that can be attributed to the single bounce mechanism at the rough ice-water boundary (Engram et al., 2013; Atwood et al., 2015; Antonova et al., 2016). Due to this contrasting behaviour, the identification and characterisation of the meltwater features only based on backscatter intensity is not straightforward. Several of the observed lakes show for example similar NRCS as their surrounding for long periods, and even during the freezing/melting processes (e.g. Fig. 5 or Fig. 7).

Backscatter intensity therefore may not be sufficient to fully characterise meltwater processes. Coherence, however, provides additional dynamic information as it helps assessing the degree of stability of the ice cover between two acquisitions. Coherence is an important property estimated from interferometric computation of Sentinel-1 SLC data. For repeat-pass acquisition such as Sentinel-1, a loss of coherence mainly reveals the extent of a surface change (Zebker and Villasenor, 1992). However, with substantial microwave penetration depths in snow/firn, coherence variations indicate changes in scattering properties. Coherence losses consequently may be due to changes in volume scattering (Zebker and Hoen, 2000) or subsurface processes. Low coherence between interferometric images can therefore indicate altering scattering properties (e.g. a strong snowfall or an intense melt event), but also changes in ice-water interface due to refreezing meltwater lakes (Antonova et al., 2016) where refreezing may result in a gradually increase in coherence. Ice and snow areas are typically characterised by a high coherence, while meltwater lakes show a low coherence due to the constantly changing ice/water interface. This added value of coherence is shown, for example, in Fig. 4 and 5, where the coherence provides more insight into the temporal dynamics of the lakes than the NRCS images alone. The change from disk shaped low coherence patterns to ring shaped patterns (Fig. 4) for example provide an important indicator of the gradual refreezing patterns (i.e more refreezing in the centre than at the edges). These results correspond to the study of Antonova et al. (2016), where the melting and refreezing of lake ice could be observed by using both backscatter intensity and coherence image time series.

Also the interferometric phase has shown to be a useful indicator for assessing meltwater dynamics when the interferometric images show a high coherence. Local volume changes caused by gradual refreezing may be hard to quantify because the refreezing process may change the ice-water interface constantly, affecting the quality of the interferogram. However, the deformation due to instant meltwater events, such as drainage and collapse, may be captured, if the fringe pattern in the lake area appears highly distinct to the surroundings affected by tidal displacement. Within this context, we identified two advantages of the phase fringes over the NRCS and coherence alone: i) an easier detection of stable ice or refrozen than coherence and backscatter intensity and ii) the detection of relative motion related due to uplift and subsidence events as

https://doi.org/10.5194/tc-2021-169
Preprint. Discussion started: 12 July 2021

a result of lake drainage or lake filling. The first advantage is clear in Figs. 4-7, where the phase patterns allow additional interpretation of the refreezing patterns which cannot be revealed by the coherence or backscatter intensity alone. The second advantage is in Fig. 6, where we could estimate the presence a uplift event due to lake drainage.

Although the InSAR analysing approach shows a clear potential for assessing meltwater lake dynamics, it also comes with challenges and drawbacks. First, it requires high coherence between image pairs to allow a meaningful interpretation of metwater lake dynamics (e.g. as in Fig. 7). When the revisit cycle for SLC data is low or when the surface changes due to other processes (e.g. strong snowfall event), the interpretation of coherence and phase changes may be limited. On Amery, the Sentinel-1 mission has a 6-day revisit, whilst the revisit period on the RBIS is 12 day. Due to this difference, the lake processes are better observed on Amery than the RBIS. Second, the interpretation of phase change can only be done relative to the displacement of the lake surroundings in the line-of-sight. As the meltwater lakes typical develop on locations with strong ice and/or tidal displacement, interpretation should be done relative to that displacement which makes interpretation more complicated.

5 Conclusions

The goal of this study was to provide an insight on the capabilities of coherent and incoherent SAR data to assess the meltwater dynamics on ice shelves. Four regions with intense melt on two ice shelves in Antarctica have been analysed based on C-band Sentinel-1 SAR data and corresponding available Landsat 8 imagery. The spatial and temporal inspection of the meltwater features conveyed that the backscatter intensity allows identification of the freezing and melting events as the lakes show an increase of the intensity due to the water-ice boundary when the lake is not completely frozen. The extent of such dynamics however depends on the morphology of the lake and on the weather conditions. A generalisation on of the meltwater detection is however not straightforward as meltwater lakes often show similar backscatter intensity values to their surroundings. In such context, InSAR information, i.e. the coherence and the interferogram phases, can be useful to increase the confidence of such delineation especially during the freezing and melting period. Besides, such indicators can be additionally exploited to infer the stability of the lake ice and its connection with the ice layer in the ground. The coherence in this context allows to detect changes in the ice-water interface which shows clearer patterns than the backscatter intensity alone, while the interferograms can reveal refreezing patterns. The interferograms allow moreover to detect the relative displacement of the lakes which can be useful to detect abrupt lake drainage or filling.

The paper also points at the limitations that due to the 12-days Sentinel-1 repeat cycle over the RBIS, is it hardly sufficient to provide an inter-annual observation and comparison. A revisit larger than 6 days may greatly reduce the coherence and compromise the quality of the (complicated) unwrapping step over the ice shelf. Several InSAR products completely impaired by weather events, in winter, most likely attributable to precipitations and wind, and by fast surface changes in summer, were found as a result.

https://doi.org/10.5194/tc-2021-169
Preprint. Discussion started: 12 July 2021

In conclusion, this study shows a promising possibility to monitor the local dynamics of specific water features on the ice shelves by using InSAR, potentially paving the way towards dedicated Sentinel-1 meltwater products that could facilitate the study of ice shelves in a changing climate.

Code availability. The DORIS software used to process Sentinel-1 SLC data is available at http://doris.tudelft.nl.

Data availability. The TanDEM-X data used for geo-coding the InSAR SLC products on the RBIS are available at https://doi.org/10.1594/pangaea.868109.

Author contributions. SL developed the idea of this study and provided access to the mapped locations of the meltwater ponds on the RBIS and TanDEM-X data. PLD provided expertise in processing and interpreting InSAR data. WL was responsible for managing the data, processing the data with DORIS, re-processing and re-analysing the results, producing the figures, and providing the manuscript.

Competing interests. The authors declare they have no conflict of interest.

Acknowledgements. We are grateful for the DORIS development team at TU Delft. We acknowledge Copernicus Open Access Hub for providing Sentinel-1 SLC data, and Google Earth Engine for providing Landsat 8 and Sentinel-1 GRD images.

DEM for visualisation is provided by the Byrd Polar and Climate Research Center and the Polar Geospatial Center under NSF-OPP awards 1543501, 1810976, 1542736, 1559691, 1043681, 1541332, 0753663, 1548562, 1238993 and NASA award NNX10AN61G. Computer time is provided through a Blue Waters Innovation Initiative. The DEM is produced using data from DigitalGlobe, Inc.

We would also like to thank Dr Lorenzo Iannini and Malte Manne for proof-reading and discussion.

https://doi.org/10.5194/tc-2021-169
Preprint. Discussion started: 12 July 2021

References

Antonova, S., Duguay, C., Kääb, A., Heim, B., Langer, M., Westermann, S., and Boike, J.: Monitoring Bedfast Ice and Ice Phenology in Lakes of the Lena River Delta Using TerraSAR-X Backscatter and Coherence Time Series, Remote Sensing, 8, 903, https://doi.org/10.3390/rs8110903, 2016.

Atwood, D. K., Gunn, G. E., Roussi, C., Wu, J., Duguay, C., and Sarabandi, K.: Microwave Backscatter From Arctic Lake Ice and Polarimetric Implications, IEEE Transactions on Geoscience and Remote Sensing, 53, 5972–5982, https://doi.org/10.1109/TGRS.2015.2429917, 2015.

Banwell, A. F., MacAyeal, D. R., and Sergienko, O. V.: Breakup of the Larsen B Ice Shelf triggered by chain reaction drainage of supraglacial lakes, Geophysical Research Letters, 40, 5872–5876, https://doi.org/10.1002/2013gl057694, 2013.

Bell, R. E., Banwell, A. F., Trusel, L. D., and Kingslake, J.: Antarctic surface hydrology and impacts on ice-sheet mass balance, Nature Climate Change, 8, 1044–1052, https://doi.org/10.1038/s41558-018-0326-3, http://www.nature.com/articles/s41558-018-0326-3, 2018.

Benedek, C. L. and Willis, I. C.: Winter drainage of surface lakes on the Greenland Ice Sheet from Sentinel-1 SAR imagery, The Cryosphere, 15, 1587–1606, https://doi.org/10.5194/tc-15-1587-2021, 2021.

Copernicus: Open Access Hub, https://scihub.copernicus.eu, accessed 2 Nov. 2017, 2017.

Dirscherl, M., Dietz, A. J., Kneisel, C., and Kuenzer, C.: A Novel Method for Automated Supraglacial Lake Mapping in Antarctica Using Sentinel-1 SAR Imagery and Deep Learning, Remote Sensing, 13, https://doi.org/10.3390/rs13020197, 2021.

Dunmire, D., Lenaerts, J. T. M., Banwell, A. F., Wever, N., Shragge, J., Lhermitte, S., Drews, R., Pattyn, F., Hansen, J. S. S., Willis, I. C., Miller, J., and Keenan, E.: Observations of Buried Lake Drainage on the Antarctic Ice Sheet, Geophysical Research Letters, 47, e2020GL087 970, https://doi.org/https://doi.org/10.1029/2020GL087970, 2020.

Engram, M., Anthony, K. W., Meyer, F. J., and Grosse, G.: Characterization of L-band synthetic aperture radar (SAR) backscatter from floating and grounded thermokarst lake ice in Arctic Alaska, The Cryosphere, 7, 1741–1752, https://doi.org/10.5194/tc-7-1741-2013, 2013.

Fahnestock, M., Bindschadler, R., Kwok, R., and Jezek, K.: Greenland Ice Sheet Surface Properties and Ice Dynamics from ERS-1 SAR Imagery, Science, 262, 1530–1534, https://doi.org/10.1126/science.262.5139.1530, 1993.

Hanssen, R. F.: Radar Interferometry, Springer Netherlands, https://doi.org/10.1007/0-306-47633-9, 2001.

Hirose, T., Kapfer, M., Bennett, J., Cott, P., Manson, G., and Solomon, S.: Bottomfast Ice Mapping and the Measurement of Ice Thickness on Tundra Lakes Using C-Band Synthetic Aperture Radar Remote Sensing, JAWRA Journal of the American Water Resources Association, 44, 285–292, https://doi.org/10.1111/j.1752-1688.2007.00161.x, 2008.

Howat, I. M., Porter, C., Smith, B. E., Noh, M.-J., and Morin, P.: The Reference Elevation Model of Antarctica, The Cryosphere, 13, 665–674, https://doi.org/10.5194/tc-13-665-2019, 2019.

Kingslake, J., Ely, J. C., Das, I., and Bell, R. E.: Widespread movement of meltwater onto and across Antarctic ice shelves, Nature, 544, 349–352, https://doi.org/10.1038/nature22049, 2017.

Lenaerts, J. T. M., Lhermitte, S., Drews, R., Ligtenberg, S. R. M., Berger, S., Helm, V., Smeets, C. J. P. P., van den Broeke, M. R., van de Berg, W. J., van Meijgaard, E., Eijkelboom, M., Eisen, O., and Pattyn, F.: Meltwater produced by wind–albedo interaction stored in an East Antarctic ice shelf, Nature Climate Change, 7, 58–62, https://doi.org/10.1038/nclimate3180, 2016.

https://doi.org/10.5194/tc-2021-169
Preprint. Discussion started: 12 July 2021

Miles, K. E., Willis, I. C., Benedek, C. L., Williamson, A. G., and Tedesco, M.: Toward Monitoring Surface and Subsurface Lakes on the Greenland Ice Sheet Using Sentinel-1 SAR and Landsat-8 OLI Imagery, Frontiers in Earth Science, 5, https://doi.org/10.3389/feart.2017.00058, 2017.

Nagler, T., Rott, H., Ripper, E., Bippus, G., and Hetzenecker, M.: Advancements for Snowmelt Monitoring by Means of Sentinel-1 SAR, Remote Sensing, 8, https://doi.org/10.3390/rs8040348, 2016.

Selmes, N., Murray, T., and James, T. D.: Characterizing supraglacial lake drainage and freezing on the Greenland Ice Sheet, The Cryosphere Discussions, 7, 475–505, https://doi.org/10.5194/tcd-7-475-2013, 2013.

Spergel, J. J., Kingslake, J., Creyts, T., van Wessem, M., and Fricker, H. A.: Surface meltwater drainage and ponding on Amery Ice Shelf, East Antarctica, 1973–2019, Journal of Glaciology, p. 1–14, https://doi.org/10.1017/jog.2021.46, 2021.

Torres, R., Snoeij, P., Geudtner, D., Bibby, D., Davidson, M., Attema, E., Potin, P., Rommen, B., Floury, N., Brown, M., Traver, I. N., Deghaye, P., Duesmann, B., Rosich, B., Miranda, N., Bruno, C., L'Abbate, M., Croci, R., Pietropaolo, A., Huchler, M., and Rostan, F.: GMES Sentinel-1 mission, Remote Sensing of Environment, 120, 9–24, https://doi.org/10.1016/j.rse.2011.05.028, 2012.

Ulaby, F. T., Moore, R. K., and Fung, A. K.: Microwave Remote Sensing Active and Passive, The Artech House Remote Sensing Library, 1981.

Williamson, A. G., Arnold, N. S., Banwell, A. F., and Willis, I. C.: A Fully Automated Supraglacial lake area and volume Tracking ("FAST") algorithm: Development and application using MODIS imagery of West Greenland, Remote Sensing of Environment, 196, 113–133, https://doi.org/10.1016/j.rse.2017.04.032, 2017.

Zebker, H. and Hoen, E. W.: Penetration depths inferred from interferometric volume decorrelation observed over the Greenland Ice Sheet, IEEE Transactions on Geoscience and Remote Sensing, 38, 2571–2583, https://doi.org/10.1109/36.885204, 2000.

Zebker, H. and Villasenor, J.: Decorrelation in interferometric radar echoes, IEEE Transactions on Geoscience and Remote Sensing, 30, 950–959, https://doi.org/10.1109/36.175330, 1992.